

Phase retrieval from angular streaking of XUV atomic ionization

Anatoli S. Kheifets¹, Rickson Wielian¹, Igor A. Ivanov², Anna Li Wang³, Agostino Marinelli³, and James P. Cryan³

¹*Research School of Physics, The Australian National University, Canberra ACT 2601, Australia**

²*Center for Relativistic Laser Science, Institute for Basic Science (IBS), Gwangju 61005, South Korea and*

³*Stanford PULSE Institute SLAC National Accelerator Laboratory, Menlo Park, CA 94025 USA*

(Dated: March 8, 2022)

We demonstrate an accurate phase retrieval of XUV atomic ionization by streaking the photoelectron in a circularly polarized IR laser field. The streaking phase can then be converted to the atomic time delay containing the Wigner and continuum-continuum components. Our demonstration is based on a numerical solution of the time-dependent Schrödinger equation. We test this technique using the hydrogen atom ionized by an isolated attosecond XUV pulse across a wide range of photon energies. In parallel, we run a series of RABBITT simulations and demonstrate equivalence of the phase and timing information provided by the two methods. This validates the proposed technique and makes it a useful tool that can be applied to a broad range of atomic and molecular targets exposed to XUV radiation from novel free-electron laser sources.

PACS numbers: 32.80.Rm 32.80.Fb 42.50.Hz

Angular streaking of extreme ultraviolet (XUV) atomic ionization with a circularly polarized IR laser radiation has become a useful tool for characterizing isolated attosecond pulses (IAP) from free-electron laser (FEL) sources. First suggested theoretically [1–4], this method has been implemented in practice for a shot-to-shot characterization of IAP at FEL [5, 6]. Angular streaking of XUV ionization combines elements of the two previously developed techniques: attosecond angular streaking known as the attoclock [7–9] and the attosecond streak camera [10–17]. It is analogous to the attosecond streak camera in that XUV pulses are the primary source of ionization while it is common to the attoclock in that the ionized electrons interact with a circularly polarized laser field which alters the photoelectron momentum distribution (PMD). This alteration is most vividly observed in the plane perpendicular to the laser propagation direction. The difference with the attoclock is that the latter is a self-referencing technique where both tunneling ionization and steering are driven by the same elliptical infrared (IR) laser pulse. In its original form [2–6], angular streaking of XUV ionization was considered in an intense IR laser field and analyzed within the strong field approximation (SFA) [18]. An alternative view within the lowest order perturbation theory (LOPT) [19–21] considers IR streaking as an interference phenomenon which opens a natural access to the streaking phase Φ_S . The latter is typically decomposed into the XUV ionization phase (or Wigner phase) and the continuum-continuum (CC) phase from the IR interaction. These two phases can be converted to the corresponding time delay components, which add up to the atomic time delay. This delay is often interpreted as the time it takes for the electron to be photoionized plus the time it takes for the measurement process to occur. This timing analysis

has been used to determine the attosecond time delay in photoemission from atoms [22] and solid surfaces [23]. The latter seminal works opened up the rapidly growing field of attosecond chronoscopy of photoemission [24–26]. While angular streaking of XUV ionization is conceptually similar to the analogous process utilizing a linearly polarized IR field, its phase retrieval capability has not been explored so far.

In this Letter, we propose a phase retrieval method based on angular streaking of XUV ionization. This method is applicable over a wide range of photoelectron energies right from the ionization threshold and exceeding it many times. We demonstrate the accuracy of the proposed technique by considering the hydrogen atom driven by a femtosecond XUV pulse across a wide range of carrier frequencies. Our demonstration is based on a numerical solution of the time-dependent Schrödinger equation (TDSE). It is verified through comparison with the well established RABBITT (reconstruction of attosecond beating by interference of two-photon transitions) technique. Both methods are shown to provide equivalent phase and timing information. This validates the proposed technique and makes it a useful tool that can be applied to a broad range of atomic and molecular targets exposed to XUV radiation from novel free-electron laser sources.

An interference character of IR streaking of XUV ionization is illustrated in the left panel of Fig. 1. There are three ionization channels marked (d), (a) and (e) leading to the same final state with the photoelectron energy E . While the direct channel (d) contains an unassisted XUV ionization, two other channels are aided by an IR absorption (a) or emission (e). For these three channels to interfere, the spectral width of the XUV pulse should be large enough to accommodate the $\pm\omega$ processes. In the time domain, this means that the XUV pulse is shorter than the laser period. Such a spectrum is illustrated in the right panel of Fig. 1 which corresponds to ionization of the hydrogen atom at the XUV and IR photon energies

*Electronic address: A.Kheifets@anu.edu.au

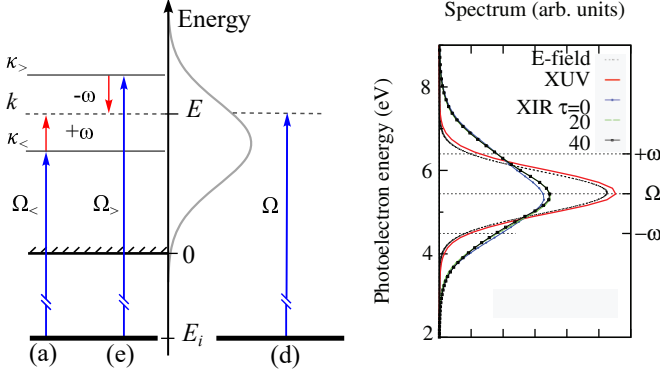


FIG. 1: Left: Schematic representation of IR streaking of XUV ionization. The first order direct process (d) and the second order processes aided by an IR photon absorption (a) and emission (e) are labeled accordingly (adopted from [20]). Right: photoelectron spectrum of H driven by XUV and XIR fields is overlapped with the Fourier transform of the electric field.

$\Omega = 0.7$ au and $\omega = 0.038$ au, respectively, while FWHM of the XUV pulse is set to 2 fs. The photoelectron spectrum of an unassisted XUV photoionization (process d) is an exact replica of the Fourier transform of the electric field shifted by the ionization potential. Meanwhile, the photoelectron spectrum of XUV+IR ionization (XIR for brevity) is significantly broadened by the second-order (a) and (e) processes.

The proposed phase retrieval of angular streaking of XUV ionization is based on the following consideration. We apply the SFA and write the photoionization amplitude as [27]

$$b(\mathbf{k}, \tau) = i \int_{t_0}^{\infty} dt E_x(t - \tau) D_x[\mathbf{k} - \mathbf{A}(t)] e^{-i\Phi(t)}. \quad (1)$$

Here the electric field of the XUV pulse E_x is advancing the streaking pulse by the time τ . The streaking field is described by its vector potential

$$\mathbf{A}(t) = - \int_0^t \mathbf{E}(t') dt' = A_0 \cos(\omega t) \hat{\mathbf{x}} + A_0 \sin(\omega t) \hat{\mathbf{y}},$$

while the photoelectron momentum is confined to the polarization plane $\mathbf{k} = k \cos \phi \hat{\mathbf{x}} + k \sin \phi \hat{\mathbf{y}}$, where ϕ is the emission angle.

The exponential term contains the so-called Volkov phase

$$\Phi(t) = \frac{1}{2} \left[\int_t^{\infty} dt' [\mathbf{k} - \mathbf{A}(t')]^2 - k_0^2 t \right], \quad (2)$$

in which the photoelectron energy in the absence of streaking $E_0 = k_0^2/2 = \Omega - I_p$. This phase can be estimated by the saddle point method (SPM) which selects the most probable photoelectron trajectories leaving the atom at the time t_{st} and keeping the phase stationary:

$$\Phi'(t_{st}) = \frac{1}{2} |\mathbf{k} - \mathbf{A}(t_{st})|^2 - E_0 = 0 \quad (3)$$

We assume that the XUV pulse is short relative to the IR pulse and shifted relative to its peak position by the time τ . Under these conditions, Eq. (3) is transformed to the following *isochrone* equation [2]:

$$k^2/2 - E_0 = kA_0 \cos(\phi - \omega\tau); \quad \begin{cases} k > k_0 & \phi - \omega\tau \sim 0 \\ k < k_0 & \phi - \omega\tau \sim 180^\circ \end{cases} \quad (4)$$

Here we neglected the ponderomotive energy $U_p = A_0^2/2$ in a weak streaking field. In the above derivation it was implicitly assumed that the phase of the dipole matrix element $D[\mathbf{k} - \mathbf{A}(t)]$ does not depend on the photoelectron energy. In a more general case, this phase contains an energy dependent term

$$\arg \{D[\mathbf{k} - \mathbf{A}(t)]\} \propto \alpha |\mathbf{k} - \mathbf{A}(t)|^2/2, \quad (5)$$

where

$$\alpha = \partial \arg D(\sqrt{2E}) / \partial E \quad (6)$$

is a generalized definition of the photoelectron group delay in photoemission (see e.g. Eq. (S10) of Schultze et al. [22]). The introduction of this delay modifies the stationary phase equation:

$$\frac{1}{2} |\mathbf{k} - \mathbf{A}(t_{st})|^2 - E_0 + \frac{\alpha}{2} \frac{d}{dt} [(\mathbf{k} - \mathbf{A}(t_{st}))^2] = 0 \quad (7)$$

This leads to a modified isochrone equation

$$\begin{aligned} k^2/2 - E_0 &= kA_0 [\cos(\phi - \omega t_{st}) - \alpha \omega \sin(\phi - \omega t_{st})] \\ &\approx kA_0 \cos[\phi - \omega t_{st} + \omega \alpha] \end{aligned} \quad (8)$$

In the second line, we used the identity $b \cos x - a \sin x = \sqrt{1 + (ab)^2} \cos(x + y)$, $y = \tan^{-1}(a/b)$ and the long wavelength approximation $\omega \alpha \ll 1$ for the streaking field. Thus the isochrone acquires an additional phase shift $\omega \alpha$ which can be extracted from the photoelectron momentum distribution (PMD). In the following, we shall demonstrate that $\alpha = \tau_a$ under certain XUV and IR pulse parameters.

In Fig. 2 we display the PMD of the hydrogen atom ionized with a 2 fs XUV pulse at 6×10^{13} W/cm² and $\Omega = 0.7$ au, in the presence of a long IR pulse with $\omega = 0.038$ au ($\lambda = 1200$ nm), FWHM = 25 fs at 1.5×10^{11} W/cm². The XUV pulse is linearly polarized along the $\hat{\mathbf{x}}$ axis whereas the IR pulse is circularly polarized in the (xy) plane. The PMD is projected on this plane. The top panel of Fig. 2 exhibits the PMD obtained by SPM while the bottom panel displays the corresponding TDSE result. The latter calculation is carried out using the spherical-coordinate implicit derivatives (SCID) computer code [28]. The code was cross-checked against another numerical TDSE implementation [29], and both methods produced nearly identical results. At each XUV photon frequency, we scan the delay between the XUV pulse and the IR laser field (τ) in the range of 0 to 60 au in 7 steps. The same procedure was followed by the SPM calculation. The PMD shown in both panels of Fig. 2 correspond to $\tau = 0$.

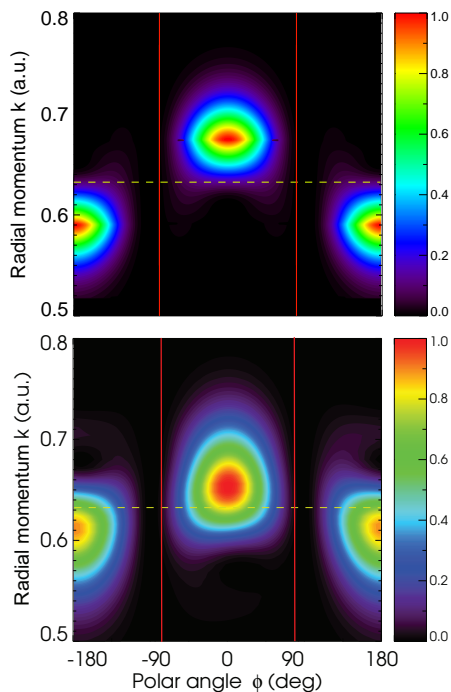


FIG. 2: PMD of the hydrogen atom in the polarization plane calculated in SPM (top) and TDSE (bottom) $\tau = 0$ calculations. The dashed horizontal line visualizes the momentum value $k_0 = \sqrt{2(\Omega - I_p)}$ from the energy conservation. The solid vertical lines define the angular integration limits.

The top panel of Fig. 2 visualizes the isochrone (4) most vividly. The PMD maxima are displaced relative to the photoelectron momentum k_0 (dashed line) by the amount $\pm A_0$. While the TDSE calculation retains this feature of Eq. (4), the PMD has a broader spread because of a finite XUV spectral width as displayed on the right panel of Fig. 1. The SPM result corresponds to a zero XUV spectral width.

The isochrone equation (4) allows, in principle, for the phase extraction from the angular resolved PMD(k, ϕ). However, the realistic PMD has a much broader spread because of a finite XUV spectral width. To deal with this spread, we integrate the PMD exhibited in Fig. 2 over the angular intervals spanning the upwards (+) and downwards (-) shifted lobes which are centered at $\phi = 0$ and $\pm 180^\circ$, respectively. We carry out this procedure at several fixed increments of the XUV/IR delay τ . The corresponding radial momentum profiles $P(k, \tau)$ are shown in the top panel of Fig. 3 for the angular integration range $-90^\circ < \phi < 90^\circ$ corresponding to the k_+ solution. The analogous profiles corresponding to the k_- solution mirror closely that of the k_+ one. The centers of the momentum profiles $P(k, \tau)$ are fitted with a Gaussian function. Thus determined peak positions k_\pm are then used to obtain the isochrone phase offset:

$$k_\pm^2/2 - E_0 = \pm k A_0 \cos(\phi - \omega\tau - \Phi_S), \quad (9)$$

as illustrated in the bottom panel of Fig. 3.

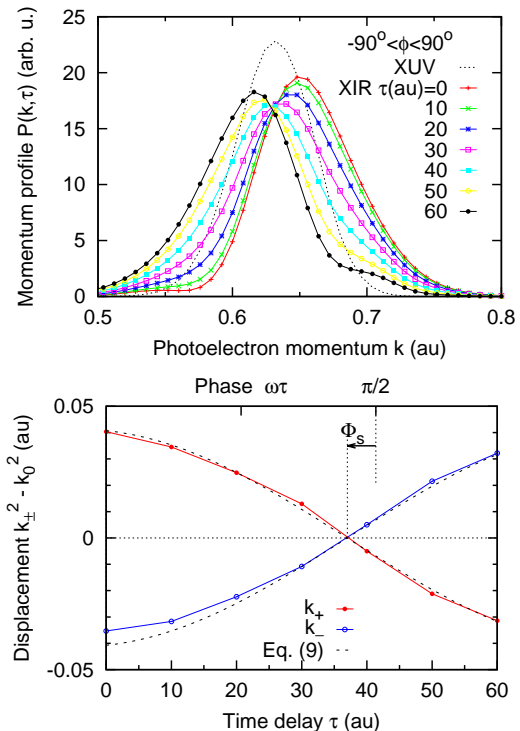


FIG. 3: Top: radial momentum profiles after angular integration in the $-90^\circ < \phi < 90^\circ$ range (between the vertical lines drawn in the bottom panel of Fig. 2). The peaks of $P(k, \tau)$ define the shifted photoelectron momentum k_+ . Bottom: radial momentum displacements $k_\pm^2/2 - k_0^2/2$ are shown at various XUV/IR delays τ . The dashed line represents the fit with Eq. (9). The arrow indicates the streaking phase Φ_S .

This procedure of the streaking phase extraction was repeated at various XUV photon frequencies and the results are summarized in Fig. 4. To benchmark our method, we resort to the RABBITT technique. Even though this technique employs a linearly polarized weak IR field, it returns the needed phase information which can be used as a solid reference. RABBITT usually analyses the photoelectron spectrum but direct PMD mapping can also be achieved [30, 31]. In the present study, we ran a series of RABBITT calculations on hydrogen at the same IR intensity and various wavelengths λ . Numerical details of these calculations can be found in preceding works [32, 33]. From these simulations, we obtain the RABBITT phase Φ_R by fitting the angular integrated photoelectron spectra at various τ with the following expression:

$$S_{2q}(\tau) = A + B \cos[2\omega\tau - \Phi_R(E)] \quad (10)$$

Here the sideband index $2q$ defines the photoelectron energy $E = 2q\omega - I_p$. We note that the amplitudes of the RABBITT peaks (10) oscillate with twice the laser frequency $\propto 2\omega\tau$ and the atomic time delay is defined as $\tau_a = \Phi_R/(2\omega)$. In the meantime the streaking signal (9) contains the $\propto \omega\tau$ oscillation and we expect the atomic time delay to be expressed as $\tau_a = \Phi_S/\omega$. Therefore, we make a comparison of the RABBITT phase Φ_R

with twice the streaking phase $2\Phi_S$. This comparison is shown in the top panel of Fig. 4. The error bars in the figure indicate the accuracy of the fitting procedure with the isochrone and RABBITT equations (4) and (10), respectively, using the Marquardt-Levenberg nonlinear algorithm. We observe in Fig. 4 a rather weak dependence of the RABBITT phase on λ and a very close agreement between Φ_R and $2\Phi_S$. This agreement is the central result of the present work which demonstrates the accuracy of the angular streaking phase extraction from near threshold to fairly large photoelectron energies.

The phase of the angular integrated RABBITT signal can be converted directly to the atomic time delay as $\tau_a = \Phi_R/(2\omega)$. Similarly, the streaking phase can be converted to the time delay as $\tau_a = \Phi_S/\omega$. This conversion is shown on the bottom panel of Fig. 4. As the hydrogen atom is free from many-electron correlation and resonances, we can test the separability of the atomic time delay into the of the Wigner and the CC components. In photoemission of hydrogen, the Wigner time delay τ_W can be calculated as the energy derivative of the Coulomb elastic scattering phase in the partial p -wave. The hydrogenic CC correction τ_{cc} is digitized from Fig. (9) of [20]. The latter is limited to the lowest photoelectron energy of 10 eV and the fixed IR wavelengths $\lambda = 0.8 \mu\text{m}$ and $2 \mu\text{m}$. We apply the analytic fit $N/E^n(a \log E + b)$ at each wavelength. Then we interpolate the corresponding coefficients to $\lambda = 1.2 \mu\text{m}$ and extrapolate this set to lower photoelectron energies of our interest. The calculated atomic time delay is sandwiched nicely between the Coulomb time delay augmented by CC corrections at various λ . Thus the separability of the atomic time delay into the Wigner and CC components is confirmed, as was the case for outer shells of noble gas atoms (see e.g. [32, 34]). As an additional test, we run a set of analogous streaking and RABBITT calculations with the Yukawa atom in which the Coulomb potential is screened as $(Z/r)\exp(-r/a)$, where $Z = 2.785$ and $a = 0.5$, thus maintaining the hydrogen atom ionization potential. Both the streaking and RABBITT phases vanish in the Yukawa atom thus indicating the Coulomb origin of the atomic time delay in hydrogen. In addition, the streaking phase vanishes once the same phase extraction method is applied to the SPM data. This assures the accuracy of our technique.

In conclusion, we demonstrate an accurate retrieval of the streaking phase Φ_S from XUV atomic ionization in the presence of a circularly polarized IR laser field. For this purpose, we introduce Φ_S into the isochrone equation (4) derived in [2]. The modified isochrone (8) has two phase shifts. One is due to the XUV/IR delay $\omega\tau$ which can be controlled by an incremented displacement of the short XUV pulse relative to the long IR pulse. An additional term $\omega\alpha$ is due to the energy dependent phase of the dipole ionization amplitude (6). Our numerical simulations on hydrogen indicate that such an extracted phase can be converted directly to the atomic time delay similarly to the analogous conversion of the phase of the

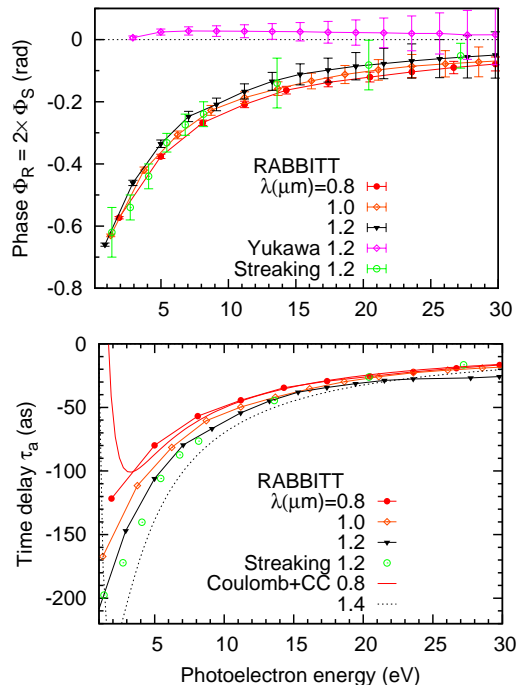


FIG. 4: Top: the RABBITT phase Φ_R as extracted from Eq. (10) is compared with the twice the streaking phase $2\Phi_S$ obtained from the isochrone ansatz Eq. (4). Bottom: the RABBITT time delay $\tau_a = \Phi_R/(2\omega)$ is compared with the Coulombic Wigner time delay augmented by the CC correction at various wavelengths λ .

RABBITT oscillation $\Phi_S = \omega\tau_a = \Phi_R/2$. This demonstration is not by any means obvious given a noticeable deviation of a realistic PMD from simplistic predictions of the saddlepoint method. Simplicity of the hydrogen atom allows us to break down the atomic time delay τ_a into the Wigner τ_W and τ_{cc} . In the absence of resonances [35], these components are responsible respectively for the time it takes for the electron to be photoionized and the time it takes for the measurement process. This interpretation was questioned recently for the Coulombic systems [36] but seems to be confirmed by the present study.

The proposed phase retrieval from angular streaking of XUV ionization can be used in measurements from XFEL sources. Experimentally, we need to measure PMD and to extract the photoelectron group delay on a single shot basis due to timing jitter inherent to the stochastic nature of XFEL radiation. Rather than systematically varying the XIR delay, we can use a reference of a second ionization state in the same target or ionization from an additional, reference target mixed with the original target. The reference and target photolines are produced by the same XUV pulse, so they share a common global streaking angle. Their difference in streaking angle will give $\tau_a - \tau_r$, where τ_r is the reference EWP group delay. If we choose a reference photoline that is much higher in energy, for example above 40 eV, and has a clear contin-

uum, then τ_r will be negligible. This technique has been implemented and analyzed in the SFA framework [37], where the radial ansatz Eq. (9) can be used to directly read the streaking angle on a single-shot basis.

As a possible application of the proposed technique, photoemission from inner atomic shells can be considered. Energy resolved spin-orbit doublets are convenient targets with built-in referencing, allowing inherent subtraction of the streaking contributions from τ , XUV pulse phase, and continuum-continuum coupling. Such accurate determination of the Wigner phase and time delay will shed new light on correlation induced attosecond ionization dynamics. As the potential target for such a measurement, the $3d$ shell of the Xe atom can be considered where the spin-split $3d_{3/2,5/2}$ components

display a strong correlation induced modification of the photoionization cross-section and angular anisotropy β parameter [38]. To account for this process, electron correlation driven channel-coupling effects between the spin-orbit split channels must be included [39].

Serguei Patchkovskii is acknowledged for placing his SCID TDSE code at author's disposal. Resources of National Computational Infrastructure facility (NCI Australia) have been employed. I.A.I acknowledges support from the Institute for Basic Science under the grant IBS-R012-D1. JPC, AM and ALW were supported by the U.S. Department of Energy (DOE), Office of Science, Office of Basic Energy Sciences (BES), Chemical Sciences, Geosciences, and Biosciences Division (CSGB).

-
- [1] Z. X. Zhao, Z. Chang, X. M. Tong, and C. D. Lin, *Circularly-polarized laser-assisted photoionization spectra of argon for attosecond pulse measurements*, Opt. Express **13**(6), 1966 (2005).
- [2] A. K. Kazansky, A. V. Bozhevolnov, I. P. Sazhina, and N. M. Kabachnik, *Interference effects in angular streaking with a rotating terahertz field*, Phys. Rev. A **93**, 013407 (2016).
- [3] S. Li, Z. Guo, R. N. Coffee, K. Hegazy, Z. Huang, A. Natan, T. Osipov, D. Ray, A. Marinelli, and J. P. Cryan, *Characterizing isolated attosecond pulses with angular streaking*, Opt. Express **26**(4), 4531 (2018).
- [4] A. K. Kazansky, I. P. Sazhina, and N. M. Kabachnik, *Fast retrieval of temporal characteristics of fel pulses using streaking by thz field*, Opt. Express **27**(9), 12939 (2019).
- [5] N. Hartmann, G. Hartmann, R. Heider, M. S. Wagner, M. Ilchen, J. Buck, A. O. Lindahl, C. Benko, J. Grüner, J. Krzywinski, et al., *Attosecond time-energy structure of x-ray free-electron laser pulses*, Nature Photonics **12**, 215 (2018).
- [6] J. Duris, S. Li, T. Driver, E. G. Champenois, J. P. MacArthur, A. A. Lutman, Z. Zhang, P. Rosenberger, J. W. Aldrich, R. Coffee, et al., *Tunable isolated attosecond x-ray pulses with gigawatt peak power from a free-electron laser*, Nature Photonics **14**, 30 (2020).
- [7] P. Eckle, M. Smolarski, P. Schlup, J. Biegert, A. Staudte, M. Schoffler, H. G. Muller, R. Dorner, and U. Keller, *Attosecond angular streaking*, Nat. Phys. **4**, 565 (2008).
- [8] P. Eckle, M. Smolarski, P. Schlup, J. Biegert, A. Staudte, M. Schoffler, H. G. Muller, R. Dorner, and U. Keller, *Attosecond angular streaking*, Nat Phys **4**, 565 (2008).
- [9] A. N. Pfeiffer, C. Cirelli, M. Smolarski, D. Dimitrovski, M. Abu-samha, L. B. Madsen, and U. Keller, *Attoclock reveals natural coordinates of the laser-induced tunnelling current flow in atoms*, Nat Phys **8**, 76 (2012).
- [10] E. Constant, V. D. Taranukhin, A. Stolow, and P. B. Corkum, *Methods for the measurement of the duration of high-harmonic pulses*, Phys. Rev. A **56**, 3870 (1997).
- [11] J. Itatani, F. Quéré, G. L. Yudin, M. Y. Ivanov, F. Krausz, and P. B. Corkum, *Attosecond streak camera*, Phys. Rev. Lett. **88**, 173903 (2002).
- [12] E. Goulielmakis, M. Uiberacker, R. Kienberger, A. Baltuska, V. Yakovlev, A. Scrinzi, T. Westerwalbesloh, U. Kleineberg, U. Heinzmann, M. Drescher, et al., *Direct measurement of light waves*, Science **305**(5688), 1267 (2004).
- [13] R. Kienberger, E. Goulielmakis, M. Uiberacker, A. Baltuska, V. Yakovlev, F. Bammer, A. Scrinzi, T. Westerwalbesloh, U. Kleineberg, U. Heinzmann, et al., *Atomic transient recorder*, Nature **427**, 817 (2004).
- [14] V. S. Yakovlev, F. Bammer, and A. Scrinzi, *Attosecond streaking measurements*, J. Mod. Opt. **52**(2-3), 395 (2005).
- [15] U. Fröhling, M. Wieland, M. Gensch, T. Gebert, B. Schütte, M. Krikunova, R. Kalms, F. Budzyn, O. Grimm, J. Rossbach, et al., *Single-shot terahertz-field-driven x-ray streak camera*, Nature Photonics **3**, 523 (2009).
- [16] C.-H. Zhang and U. Thumm, *Streaking and Wigner time delays in photoemission from atoms and surfaces*, Phys. Rev. A **84**, 033401 (2011).
- [17] M. Ivanov and O. Smirnova, *How accurate is the attosecond streak camera?*, Phys. Rev. Lett. **107**, 213605 (2011).
- [18] X. Zhao, S. Li, T. Driver, V.-H. Hoang, A.-T. Le, J. P. Cryan, A. Marinelli, and C. D. Lin, *Characterization of single-shot attosecond pulses with angular streaking photoelectron spectra*, Phys. Rev. A **105**, 013111 (2022).
- [19] J. M. Dahlström, A. L. Huillier, and A. Maquet, *Introduction to attosecond delays in photoionization*, J. Phys. B **45**(18), 183001 (2012).
- [20] J. M. Dahlström, D. Guénot, K. Klünder, M. Gisselbrecht, J. Mauritsson, A. L. Huillier, A. Maquet, and R. Taïeb, *Theory of attosecond delays in laser-assisted photoionization*, Chem. Phys. **414**, 53 (2013).
- [21] A. Maquet, J. Caillat, and R. Taïeb, *Attosecond delays in photoionization: time and quantum mechanics*, J. Phys. B **47**(20), 204004 (2014).
- [22] M. Schultze, M. Fiess, N. Karpowicz, J. Gagnon, M. Korbman, M. Hofstetter, S. Neppl, A. L. Cavalieri, Y. Komninos, T. Mercouris, et al., *Delay in Photoemission*, Science **328**(5986), 1658 (2010).
- [23] A. L. Cavalieri, N. Müller, T. Uphues, V. S. Yakovlev, A. Baltuska, B. Horvath, B. Schmidt, L. Blümel, R. Holzwarth, S. Hendel, et al., *Attosecond spectroscopy in condensed matter*, Nature **449**, 1029 (2007).
- [24] R. Pazourek, S. Nagele, and J. Burgdorfer, *Time-resolved*

- photoemission on the attosecond scale: opportunities and challenges*, Faraday Discuss. **163**, 353 (2013).
- [25] R. Pazourek, S. Nagele, and J. Burgdörfer, *Attosecond chronoscopy of photoemission*, Rev. Mod. Phys. **87**, 765 (2015).
- [26] U. Thumm, Q. Liao, E. M. Bothschafter, F. Süßmann, M. F. Kling, and R. Kienberger, in *Photonics* (John Wiley & Sons, Ltd, 2015), chap. 13, pp. 387–441, ISBN 9781119009719, URL <https://onlinelibrary.wiley.com/doi/abs/10.1002/9781119009719.ch13>
- [27] M. Kitzler, N. Milosevic, A. Scrinzi, F. Krausz, and T. Brabec, *Quantum theory of attosecond XUV pulse measurement by laser dressed photoionization*, Phys. Rev. Lett. **88**, 173904 (2002).
- [28] S. Patchkovskii and H. Muller, *Simple, accurate, and efficient implementation of 1-electron atomic time-dependent schrödinger equation in spherical coordinates*, Computer Physics Communications **199**, 153 (2016).
- [29] I. A. Ivanov, *Evolution of the transverse photoelectron-momentum distribution for atomic ionization driven by a laser pulse with varying ellipticity*, Phys. Rev. A **90**, 013418 (2014).
- [30] S. Patchkovskii, M. J. J. Vrakking, D. M. Villeneuve, and H. Niikura, *Selection of the magnetic quantum number in resonant ionization of neon using an XUV-IR two-color laser field*, J. Phys. B **53**(13), 134002 (2020).
- [31] A. S. Kheifets, *Symmetry analysis of the photoelectron continuum in two-photon XUV + IR ionization*, Phys. Rev. A **105**, 013114 (2022).
- [32] A. W. Bray, F. Naseem, and A. S. Kheifets, *Simulation of angular-resolved RABBITT measurements in noble-gas atoms*, Phys. Rev. A **97**, 063404 (2018).
- [33] A. S. Kheifets, *Strongly resonant RABBITT on lithium*, Phys. Rev. A **104**, L021103 (2021).
- [34] I. A. Ivanov and A. S. Kheifets, *Angle-dependent time delay in two-color XUV+IR photoemission of He and Ne*, Phys. Rev. A **96**, 013408 (2017).
- [35] L. Argenti, A. Jiménez-Galán, J. Caillat, R. Taïeb, I. A. Ivanov, and F. Martín, *Control of photoemission delay in resonant two-photon transitions*, Phys. Rev. A **95**, 043426 (2017).
- [36] U. Saalmann and J. M. Rost, *Proper time delays measured by optical streaking*, Phys. Rev. Lett. **125**, 113202 (2020).
- [37] T. D. Driver *et al*, *Isolated, tunable soft x-ray attosecond pulses at μ j pulse energy from a free-electron laser*, in *7th International Conference on Attosecond Science and Technology* (University of Szeged, Hungary, 2019), URL <https://www.eli-alps.hu/indico/event/22/timetable/?print=1&start=1&end=1>
- [38] A. Kivimäki, U. Hergenhahn, B. Kempgens, R. Hentges, M. N. Piancastelli, K. Maier, A. Rüdél, J. J. Tulkki, and A. M. Bradshaw, *Near-threshold study of Xe 3d photoionization*, Phys. Rev. A **63**, 012716 (2000).
- [39] V. Radojević, D. M. Davidović, and M. Y. Amusia, *Near-threshold photoionization of the Xe 3d spin-orbit doublet: Relativistic, relaxation, and intershell interaction effects*, Phys. Rev. A **67**, 022719 (2003).